Precision Engineering 88 (2024) 117–124

Contents lists available at ScienceDirect

Precision Engineering

journal homepage: www.elsevier.com/locate/precision

Evaluation of a telescopic simultaneous ballbar in a 3-axis machine tool using a reference equipment

Raquel Acero [a,b,*], Francisco Javier Brosed [a,b], Marcos Pueo [a,b], Sergio Aguado [a,b], Juan José Aguilar [a,b], Jesús Velazquez [a,b]

[a] Aragón Institute for Engineering Research (I3A), University of Zaragoza, Zaragoza, 50018, Spain
[b] Design and Manufacturing Engineering Department, University of Zaragoza. María de Luna 3, 50018, Zaragoza, Spain

ARTICLE INFO

Handling editor: R. Leach

Keywords:
Telescopic system
Interferometry
Machine tool
Multilateration
Dimensional measurement

ABSTRACT

This paper outlines the evaluation methodology for a Telescopic Simultaneous Ballbar (TSB) developed for distance measurement using an interferometer as a reference equipment. The procedure is executed in a 3-axis machine tool, one of the final applications of the TSB that is machine tool volumetric verification. Two distinct evaluation techniques are devised, with the new virtual line approach enabling an assessment of the TSB's performance within an extended verification volume and requiring only a single alignment position for the interferometer. The measurement repeatability of the equipment is assessed and its measurement uncertainty is estimated in workshop conditions. The results reveal the flexibility of the TSB measurement process similar to that of a laser tracker and the degree of measurement accuracy, which shows values comparable to the interferometer. Consequently, the TSB could facilitate faster and more accurate machine tool verification and calibration compared to existing systems.

1. Introduction

Precision machining plays an important role in modern manufacturing. The accuracy and reliability of these machines are paramount, as even minor deviations from specified tolerances can lead to costly defects and inefficiencies. Within the field of dimensional metrology, the validation procedures applied to manufacturing systems like machine tools (MT) enable the extraction of metrological data and specific characteristics from each machine. This information serves as a basis for enhancing the machine's performance and precision by augmenting the system's operational capabilities.

The different sources of error that could affect the accuracy of a machine are divided into several groups; *quasi-static errors or kinematic errors* considered as undesired linear and angular motions when moving a single axis or relative to other axes of motion, *dynamic errors* as a response of the machine to dynamic forces that may vary with time, *static load-induced elastic errors* derived from machine tool's deformation when load is induced, and *thermal errors* as a result of thermo-elastic deformations of the machine tools and workpieces caused by various internal or external heat sources [1]. Although the different sources of error influence the machine independently, the accuracy of the machine is affected by the combined effect of all of them. For this reason, it is not advisable to compensate single error sources without taking into account the other sources of interference. The improvement in the accuracy of a machine tool can be tackled mainly from two approaches: avoiding the errors by manufacturing high-precision machines during their design and assembly [2] or compensating the effect of the errors already existing in the machine [3].

With regard to the different verification techniques, two main groups can be considered depending on how the different errors are determined: direct measurement and indirect measurement [4]. The geometric verification and calibration of MTs is extensively based on ISO 230–1 [5], which describes MT's precision analysis methods. Various groups of direct measurement techniques can be categorized based on the type of error motion being measured, linear or rotary, or the utilized measurement system [6]. These include methods based on standard systems [6], methods relying on the linear propagation of a laser and its wavelength as a reference, as well as multidimensional artefacts [7] and gravity-based methods such as levels [8]. The main advantage of direct measurement lies in providing direct information on the accuracy of the machine in each of its axes, while its main disadvantages lie both in the time required for verification and in the local correction of errors [9], as

* Corresponding author. Aragón Institute for Engineering Research (I3A), University of Zaragoza, Zaragoza, 50018, Spain.
E-mail address: racero@unizar.es (R. Acero).

https://doi.org/10.1016/j.precisioneng.2024.02.001
Received 1 November 2023; Received in revised form 31 January 2024; Accepted 2 February 2024
Available online 2 February 2024

it is not possible to extrapolate the behaviour of the measured errors to the entire working volume of the machine tool.

Verification by indirect error measurement [10], allows a mathematical, not physical, correction of the joint influence of geometrical and kinematic errors of the machine on its entire working volume, while reducing the verification time used by direct methods. It is based on the multi-axis movement of the machine to reach the measurement points both for machines with three linear axes [11,12] and five-axis including linear and rotary ones [13–17]. In any case, volumetric verification is based on an intensive error identification process for a non-linear model, based on positioning error data distributed in the working volume and an objective function of the error by indirect measurement. This type of verification is linked to the compensation capacity of the different existing control software [18,19], and the verification process can even be adapted to the machine control, the influence of environmental factors such as temperature variation [20–23], the distribution of the verification points [24] and the verification sequence [25]. Similarly, as it is an intensive process of identification by minimisation, problems such as overfitting can arise if the influence of non-geometric errors such as measurement noise, vibration or repeatability is minimised. Sometimes it is even possible to obtain a solution in which the influence of geometric errors on the volumetric error of the machine has not been characterized.

It is important to highlight the special relevance of the measurement system used in the verification process, as well as in the results obtained [1]. When dealing with the volumetric verification of machine tools, different measuring systems based on interferometry are used, the laser tracer (LC) [26,27] or the laser tracker (LT) [25,28–30]. The LC measures only the distance between its origin and the point to be measured, so it needs to measure the same point from three different positions, increasing the verification time and the influence of external factors. However, the LT provides the 3D coordinates of the point to be measured from a single position using both radial information from the interferometer and angular information from its encoders. These systems need to use multilateration techniques, the LC to obtain 3D coordinates from the radial measurement and the LT to improve the accuracy of the captured points [30–36]. Already comercialized interferometry-based measurement system for the verification of small and medium-sized machine tools is identified in Refs. [37,38], where a single-arm telescopic system including consecutive multilateration measurement cycles is used. Other instruments based on interferometry are those that allow measuring the errors in the six degrees of freedom of an axis simultaneously [39,40], so it is necessary to combine them with other measurement systems such as ball-bar or double ball-bar (DBB) to measure all the errors of a 5-axis machine [15,39,41–43]. Also the *R-tests* captures a three-dimensional error trajectory within an automated measurement cycle [44,45] using linear displacement sensors.

As an alternative, the Telescopic Simultaneous Ballbar system (TSB) developed in Ref. [46], offers the precision of interferometric systems and allows autonomous tracking of a fixed sphere, either attached to the machine tool spindle or positioned on the machine tool bed for verification of axial and rotary axes, by simultaneous contact of three lines or telescopic arms using a novel multi-point kinematic coupling [47].

The system was developed for distance measurement and was initially aimed at the verification of small and medium-sized machine tools with linear and rotary axes, but it could also be applied to the verification of coordinate measuring machines, coordinate measuring articulated arms and robots. It has been developed to measure the distance between the centre of a fixed sphere mounted on the MT spindle nose and the centre of a second sphere that is assembled on the other side of the telescopic arm and that is positioned on the MT table with a kinematic support.

As the main innovation, it allows data capture in a single cycle thanks to the simultaneous operation of the three telescopic arms, unlike other previously mentioned telescopic systems equipped with a single arm and which carry out consecutive measurement cycles by multilateration. The TSB provides similar flexibility and measurement process time as LT but improves its accuracy to levels close to those of laser interferometry, avoiding the effect of temperature variations between cycles.

To evaluate the performance of this type of equipment, standards ASME B89.4.19–2021 [48], VDI/VDE 2617- part 10 [48] or UNE-EN ISO 10360–10 [49] need to be considered. All of them establish requirements and methods for the performance evaluation of laser-based spherical coordinate measurement systems, being specially focused on laser trackers. This assessment procedures involve laser tracker measurements of points from calibrated gauges. These gauges may encompass calibrated gauge blocks, step gauges, ball bars, or other gauge types characterized by either spherical or parallel geometries, with an associated uncertainty that falls below the maximum permissible error (MPE) specified by the laser tracker manufacturer. In Ref. [50], a specially designed calibrating ball beam artefact (CBBA) for length measurement instruments is introduced. This calibration gauge serves to establish reference distances between spheres and is specifically intended for calibrating the TSB. Nonetheless, since the system is engineered to verify and calibrate machine tools, it is imperative to authenticate its functionality in real workshop conditions by comparing its performance with that of a precise reference instrument.

Therefore, this paper presents the evaluation procedure of a Telescopic Simultaneous Ballbar (TSB) with a reference interferometric equipment, being the procedure carried out in one of the target applications, a 3-axis machine tool. As a result, the measurement uncertainty of the TSB is estimated in workshop conditions.

The paper is structured as follows: Section 2 details the selection of equipment and outlines the procedure for evaluating the TSB in workshop conditions, which is conducted in the MT. This section also encompasses an explanation of the generation of the virtual test line and the definition of the uncertainty budget. Section 3 presents the outcomes of the TSB evaluation using the reference interferometric equipment in the MT, along with the estimation of the measurement uncertainty of the TSB in workshop conditions. Finally, Section 4 provides the key conclusions drawn from the study.

2. Materials and methods

The individual measurement accuracy of the TSB has been assessed, when it works and is calibrated under laboratory conditions. In addition, by simulation using the Monte Carlo method, it has been possible to obtain an estimation of the measurement uncertainty the TSB when multilateration is performed using all three telescopic arms simultaneously [51]. In this section, it is introduced the procedure developed to validate the equipment's operation under workshop conditions for machine tool verification by comparing its performance to an accurate reference instrument.

2.1. Equipment selection

Based on the previous results obtained, the TSB uncertainty value with coverage factor k = 2 obtained in laboratory conditions is under 4 μm [51]. The uncertainty budget of the TSB in workshop conditions has been analysed and estimated using the Monte Carlo method with uncertainty values (k = 2) under 5 μm for calibrated lengths ranging from 410 mm to 1041 mm.

Subsequently, a Renishaw XL-80 laser interferometer (IFM) and its environmental compensation unit with specifications outlined in Table 1 was employed as the reference instrument for assessing the TSB.

Furthermore, the equipment listed in Table 1 was also used in the testing: the TSB, its environmental compensation unit (ECU) and a three-axis ANAYAK VH1800 milling machine, in which the movement of the X axis is independent of the movements of the Y and Z axes (XFYZ configuration).

The selection of the ANAYAK VH1800 milling machine was based on

Table 1
Measurement equipment and ECU characteristics.

Devices characeristics	Value
TSB Interferometer - Attocube IDS3010	
Maximun target velocity	2 m/s
Resolution	1 p.m.
Expanded uncertainty [a] *(k = 2)*	0.3 ppm
TSB environmental compensation unit (ECU) - Attocube	
Temperature uncertainty (k = 2, 0 to 50°C)	±0.01 °C
Pressure uncertainty (k = 2, 300 to 1100 mbar*)*	±0.1 mbar
Relative humidity uncertainty (k = 2, 10 to 90 %)	±0.05 %
Interferometer -Renishaw XL-80	
Maximun target velocity	4 m/s
Linear accuracy	0.5 ppm
Linear resolution	1 nm
Expanded uncertainty[a] *(k = 2)*	0.5 ppm
Interferometer environmental compensation unit (ECU)	
Air temperature sensor uncertainty (k = 2, 0 to 40°C)	±0.07 °C
Pressure uncertainty (k = 2, 650 to 1150 mbar*)*	±0.3 mbar
Material temperature sensor uncertainty (k = 2, 0 to 50°C)	±0.07 °C

its accesibility for the experimental testing but the TSB is more suitable for verification of machine tools with proportional volumes on the three axis. Equally the system could be used for improving the MT accuracy in a specific area of the verification volume.

2.2. Evaluation procedure

Before comparing the different measurement systems, it is necessary to analyse their operating principles. While the TSB provides the 3D coordinates of the points measured in an absolute reference system specific to the equipment, the laser interferometer provides information on the error of the points, depending on the set-up carried out, through a relative reference system established at the beginning of the measurement.

Therefore, in order to compare the measurement made with a system such as the TSB against a reference system such as the laser interferometer, it is necessary to use a specific indicator. In this case, the indicator chosen is the difference in distances between all the points measured by each of the devices along a test line on the MT y-axis. This indicator has two main advantages. Firstly, a relative reference system, such as the interferometer, can be used from the measurement of the MT' axis position error. Secondly, this indicator enables the comparison between equipment with absolute reference systems, avoiding adjustment errors and the change of the measured coordinates between systems with the consequent elimination of the adjustment error that would occur when performing a least squares adjustment.

The comparison of the measurements obtained with the TSB and the reference instrument used, IFM, will provide us with information on its precision in real operating conditions and therefore on their usefulness in the volumetric verification of machine tools.

2.2.1. Experimental set-up: TSB and laser interferometer

To compare the TSB measurements with those obtained with the laser interferometer, the assembly was carried out according to Fig. 1. The reflector was mounted on the same support rod of the sphere attached to the spindle nose of the MT. In this way, the verification point is as close as possible to the sphere centre. The verification of a test line in the y-axis direction was performed simultaneously with the TSB and the IFM from predefined positions accessible to both devices. In addition, both devices have environmental compensation units, see Table 1, which compensate the wavelength of the laser beam for variations in air temperature, air pressure and relative humidity, virtually eliminating any measurement errors resulting from these variations.

To minimise possible error sources that could affect the accuracy of linear measurements with the laser interferometer, the manufacturer's recommendations have been followed. In order to avoid deadpath error,

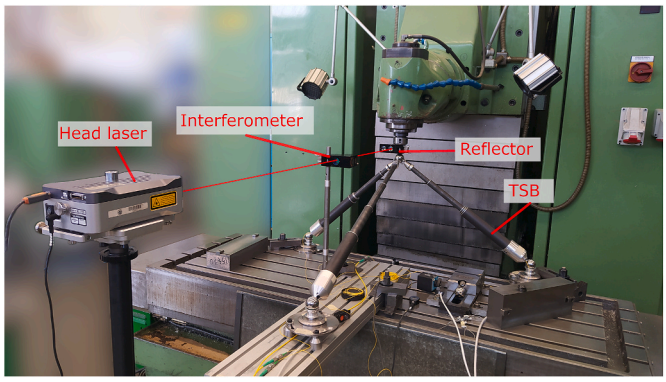

Fig. 1. Laser interferometer Renishaw XL-80 and TSB testing set-up on ANAYAK VH1800 milling machine.

the alignment has been performed by bringing the stationary and the moving optics almost in contact with each other.

Before measuring with the TSB, it is necessary to reset each of the telescopic arms. This is one of the critical points for the proper functioning of the measurement system. For this purpose, a calibrating ball beam artefact (CBBA) is used to materialise different distances, previously known, between the centres of spherical elements [50]. The CBBA materializes the calibration distances with a fixed sphere and a movable kinematic support. The movable fixture can be positioned in each of the five calibration positions of the CBBA along the measurement range of the instrument.

The procedure to be followed ensures the traceability of the system [51]. In particular, the CBBA should be placed as close as possible to the measuring area, if possible on the MT table, see Fig. 2, in order to avoid both temperature differences and unnecessary movements of the calibrated telescopic arms in their position in the machine.

For calibration, the end of the trident is placed on the fixed sphere of the CBBA and the sphere joined to the telescopic arm is connected to the CBBA via a movable fixture with a magnetic holder fixed to a kinematic self-centring support that is positioned in an intermediate calibration position of the CBBA. The system is then reset to the nominal measurement of the centre-to-centre distance of the spheres in this calibration position. Subsequently, a check is made by bringing the telescopic arm to other calibration positions, finally bringing the telescopic arm to its measuring position at the MT. The process is also repeated for the other two remaining arms.

2.2.2. Data capture and distance measurement intercomparison

The developed measurement system allows data capture in both discrete and continuous mode. In this case, the system is programmed to execute a continuous measurement and processing of the measured data.

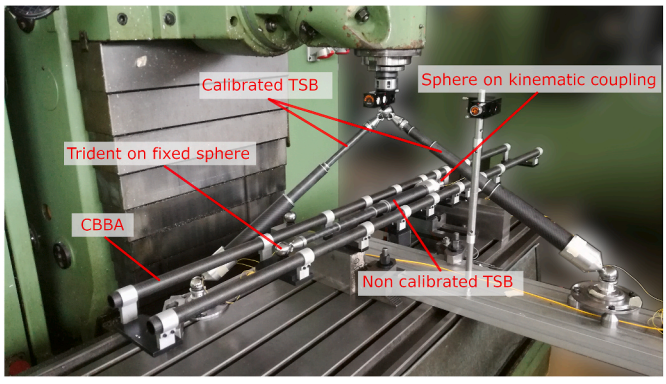

Fig. 2. TSB resetting procedure set-up with calibrating ball beam artefact (CBBA) on machine tool.

The method used to obtain discrete distances from the continuous mode distance measurement is based on point filtering using the gradient method. This method takes advantage of the difference in the measured distance over time as a consequence of the movement of the machine. If the machine is at a verification point, the difference between the measurements captured according to the sampling frequency is small. However, when the machine is moving, this difference widens, allowing the measurement to be discarded. In this way, when the machine is stable at a verification point, what is obtained for each laser is the average of a set of distances that meet the filtering criteria based on the rapid feed of the machine, stabilisation time and gap between distances. The average, maximum and minimum value are obtained for each verification distance, as well as the number of points used and the standard deviation of the measurements. From the mean distance values for the same point p, it is possible to obtain the 3D coordinates of the point using multilateration techniques.

The next step is to establish the distances between the centres of the three fixed spheres at the ends of the telescopic arms that are located in the kinematic supports positioned on the MT bed. This is a critical input parameter for the multilateration technique used in the measurement process [52]. Once the telescopic arms have been reset, they only have to be positioned in such a way that the trident of arm 1 rests on the spherical end of arm 2, the trident of arm 2 rests on the end of arm 3 and the trident of arm 3 rests on the end of arm 1 (Fig. 3), thus capturing the distances between them.

To evaluate the distance error of the TSB, a test series of ten repetitions ($n = 10$, with j from 1 to n) was carried out measuring simultaneously with the TSB and the reference equipment, interferometer in this case, a test line along the y-axis of the MT ranging from 0 to 405 mm. The details of the tests set up are shown in Fig. 1. The measurement cycle of each line took 15 min per repetition. The TSB capture frequency was 5 Hz.

Considering eleven the number of points measured, ten distances were materialized corresponding to ten ($i = 10$) calibration points, D_i, and we calculate $Da\_HPTI_{i,j}$ as the euclidean distance between the point $(i + 1)$ and the first point measured $(i = 1)$ with the TSB in the line in each repetition, see equation (1) showing method A calculation. In a second approach, method B, ten distances were generated, calculating $Db\_HPTI_{i,j}$ as the euclidean distance between the (i) point and the point $(i + 1)$ measured along the line with the TSB in each repetition, see equation (2). The reference value for each calibration distance has been obtained from the difference between the lecture of the interferómeter

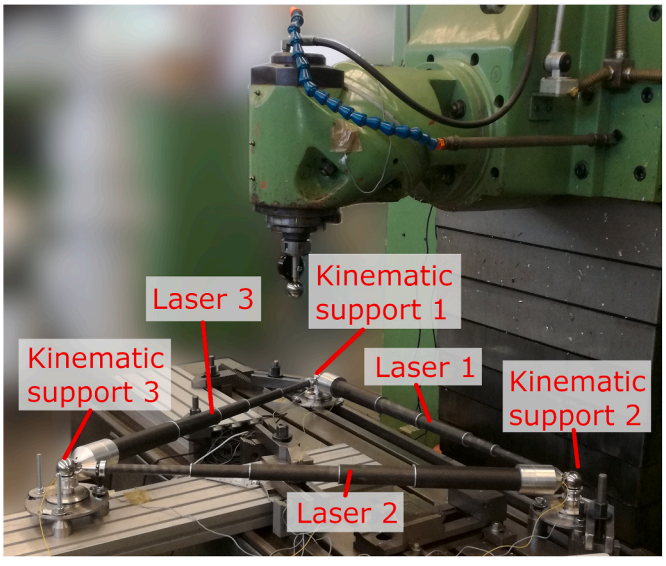

Fig. 3. Measurement of the distance between the centres of the telescopic arms on MT.

in point $(i + 1)$ and its lecture in the first point $(i = 1)$, for method A, $Da\_IFM_{i,j}$, equation (3); and as the difference between its lecture in point $(i + 1)$ and its lecture in point (i), for method B, $Db\_IFM_{i,j}$, equation (4). As happen with the TSB the distances are calculated for each repetition.

$$Da\_HPTI_{i,j} = \sqrt{\left(x_{i+1,j} - x_{1,j}\right)^2 + \left(y_{i+1,j} - y_{1,j}\right)^2 + \left(z_{i+1,j} - z_{1,j}\right)^2} \quad (1)$$

$$Db\_HPTI_{i,j} = \sqrt{\left(x_{i+1,j} - x_{i,j}\right)^2 + \left(y_{i+1,j} - y_{i,j}\right)^2 + \left(z_{i+1,j} - z_{i,j}\right)^2} \quad (2)$$

$$Da\_IFM_{i,j} = D\_IFM_{i+1,j} - D\_IFM_{1,j} \quad (3)$$

$$Db\_IFM_{i,j} = D\_IFM_{i+1,j} - D\_IFM_{i,j} \quad (4)$$

with $i = 1, \ldots, 10$, (ith calibration distance) and $j = 1, \ldots, 10$, (jth iteration).

Where $x_{i,j}$, $y_{i,j}$, and $z_{i,j}$ are the coordinates of the eleven points (until i+1) in each jth iteration and $D\_IFM_{i,j}$ is the lecture of the interferometer in each of the eleven points (until i+1) in each jth iteration.

Thus, it is possible to calculate a distance error, $D\_E_{i,j}$, perfomed by the TSB in the measurement of the distance between the points of the test line for each calibration distance i. This error corresponds to the deviation between the distance measured by the TSB and nominal distance measured by the interferometer. In this work the distance error is evaluated using the distance values obtained with method A ($Da\_E_{i,j}$) and method B ($Db\_E_{i,j}$) according to equations (5) and (6).

$$Da\_E_{i,j} = Da\_HPTI_{i,j} - Da\_IFM_{i,j} \quad (5)$$

$$Db\_E_{i,j} = Db\_HPTI_{i,j} - Db\_IFM_{i,j} \quad (6)$$

with $i = 1, \ldots, 10$, $j = 1, \ldots, 10$.

Considering a series of ten repetitions (j = 10) for the measurement of each point in the test line, a mean distance value error deviation and the standard deviation per calibration point with each distance calculation method were obtained. These error parameters will be used to evaluate the volumetric performance of the TSB in its working volume.

2.2.3. Generation of the virtual test line

An additional evaluation approach was developed considering the generation of a virtual line of verification points in the TSB working volume. In the verification procedure developed in this work, a physical test line along the y-axis of the MT is measured with the reference equipment and the TSB fixing the reference coordinate system in the kinematic support 1 (ks_1). If the position of the telescopic laser arms is changed from their initial set-up on the kinematic supports (laser 1 in ks_1, laser 2 in ks_2, laser 3 in ks_3) to a second position where the laser 1 is located in the ks_2, the laser 2 in the ks_3 and the laser 3 in the ks_1, the TSB measures the same physical line of points from a different position.

A third position of the TSB is defined with the laser 1 located in the ks_3, the laser 2 in the ks_1 and the laser 3 in the ks_2. In Fig. 4 it could be seen a 3D reconstruction of the test line using three different configurations of TSBs positioning on the kinematic supports for the simultaneous adquisition of the data.

If triangulation is performed considering the coordinate reference system in the kinematic support where laser 1 is located, a line reconstruction is obtained in a different volume from the original test line within the TSB working volumen. These coordinate reference systems are defined as virtual reference systems, $VRS_{L1,ks2}$ *and* $VRS_{L1,ks3}$ in Fig. 4.

Each virtual line is equivalent to measuring a different line rotated 120° from the previous line (Fig. 5) in the TSB coordinate reference system without changing the position of the reference equipment neither the points materialized by the MT.

In Fig. 5, it could be seen a 3D reconstruction of the test line and the two virtual lines obtained in the virtual coordinate reference systems, $VRS_{L1,ks2}$ *and* $VRS_{L1,ks3}$. The three reference systems, $RS_{L1,ks1}$, $VRS_{L1,ks2}$ *and* $VRS_{L1,ks3}$ are overlapping.

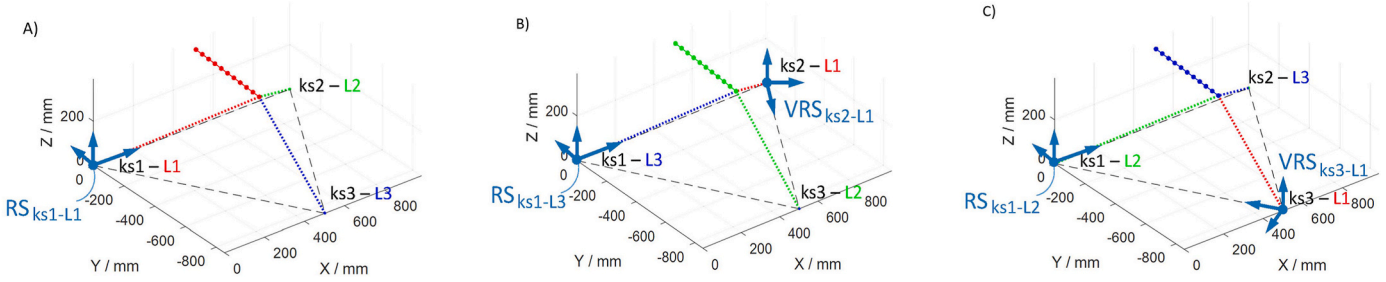

Fig. 4. 3D reconstruction of the test line. a) First configuration set up: laser 1 (L1) in kinematic support 1 (ks_1), laser 2 (L2) in (ks_2) and laser 3 (L3) in (ks_3). b) Second configuration set up: laser 1 (L1) in (ks_2), laser 2 (L2) in (ks_3) and laser 3 (L3) in (ks_1). c) Third configuration set up: laser 1 (L1) in (ks_3), laser 2 (L2) in (ks_1) and laser 3 (L3) in (ks_2). For all the cases: the coordinate reference system for the triangulation is fixed in ks_1 and L1, L2 and L3 are represented with a dot line red, green and blue respectively measuring the first calibration point. (For interpretation of the references to color in this figure legend, the reader is referred to the Web version of this article.)

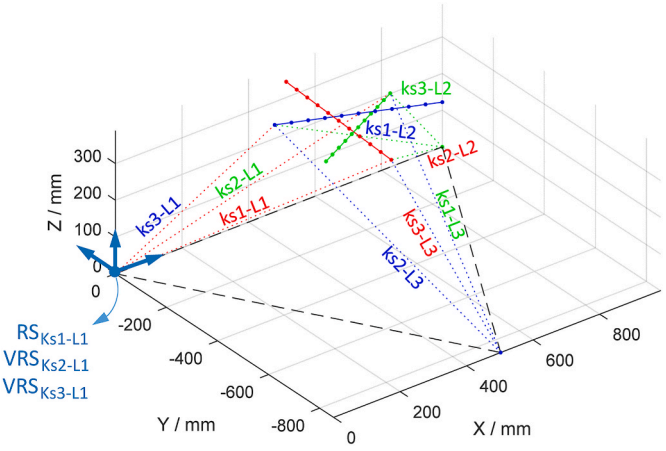

Fig. 5. 3D reconstruction of the test line and generation of the virtual test lines.

The virtual lines (blue and green) alow to verify the behaviour of the system in a wider verification volume using a single alignment position of the interferometer used as the reference instrument in this case.

The virtual distances per calibration point will be equally defined as the Euclidean distance between virtual points generated in the virtual line as defined in equations (1) and (2) for the physical test line. The deviation of the coordinates of the point will generate the corresponding distance deviation between the virtual distance measured with the TSB and the measured distance by the reference equipment, calculating the mean distance error and the standard deviation as evaluation parameters.

2.3. Measurement uncertainty estimation

In a previous work of the authors [51] the measurement uncertainty of the TSB was estimated using Monte Carlo simulation to analyse the effect of the different error sources identified in the variation of the distance measured with the TSB under workshop conditions.

In this case, the measurement uncertainty of the TSB could be assessed with experimental data by means of the comparative distance measurement carried out with the TSB and the interferometer used as a reference equipment. The uncertainty model in Eq. (7) allows estimating the TSB's measurement uncertainty based on the experimental calibration data considering the different error sources that contribute to the TSB measurement error.

(i) The uncertainty of the interferometer that is used as a reference equipment,

(ii) The standard deviation of the distance error in the calibration process, with the distance error defined as the difference between the TSB distance measurement and the interferometer one in the calibration process.

(iii) The standard deviation of the distance error in the measurement process, with the distance error defined as the difference between the TSB distance measurement and the interferometer one in the measurement process.

$$U_i = k\sqrt{\left(\frac{U_{IFM}}{k_0}\right)^2 + \frac{s_{ci}^2}{n_c} + \frac{s_{mi}^2}{n_m}} \tag{7}$$

Where.

- U_i, is the expanded uncertainty estimated for the TSB for each calibration point (with i from 1 to 10).
- k, is the coverage factor for the uncertainty estimation of the TSB, in accordance with the GUM [53].
- U_{IFM}, is the expanded uncertainty of the interferometer (see Table 1)
- k_0, is the coverage factor for the uncertainty estimation of the interferometer (see Table 1), in accordance with the GUM [53].
- s_{ci}, is the standard deviation of the TSB when measuring the distance between the calibration points of the test line in the calibration process (with i from 1 to 10).
- n_c, is the number of iterations that has been carried out when measuring the distance between the calibration points of the test line in the calibration process with the TSB (with $n_c = 10$).
- s_{mi}, is the standard deviation of the TSB when measuring distances between points in the verification process of the MT (with i from 1 to 10). It is assumed in this case $s_{ci} = s_{mi}$ due to similar measurement and calibration conditions with the TSB located in the workshop.
- n_m, is the number of repetitions performed when measuring a distance with the TSB in the verification process of the MT (with $n_m = 1$).

The TSB resolution with a value of 1 p.m., see Table 1, was considered as negligible and therefore was not included as an uncertainty contribution in equation (7).

3. Results

This section presents the results of the evaluation procedure of the TSB using an interferometer as a reference equipment, being the procedure carried out in a 3-axis machine tool. Repeatability measurement results are assessed for the TSB. The distance measurement comparison between the equipment considering the physical and virtual test lines are obtained and the error evaluation parameters are calculated. Finally, an uncertainty budget estimation for the TSB for distance measurement based on the calibration data and the experimental characterization of

the equipment is presented at the end of this section.

To evaluate the distance error of the TSB, a test series of ten repetitions was performed measuring simultaneously with the TSB and the interferometer a test line along the y-axis of the MT ranging from 0 to 405 mm. The definition of the distances along the test line was done with two different methods, A and B. In addition, it was developed in section 2.2.3 the concept of virtual test line based on the consecutive exchange of the TSBs. This methodology enables to increase the TSB verification volume without changing the configuration of the MT and the reference equipment in the MT volumetric verification process.

Table 2 shows the distance measurement comparison results of the TSB and the interferometer using distance definition method A. The results have been calculated from the data of ten iterations in eleven measurement points generating ten nominal distances, D_i, with i from 1 to 10. The interferometer and TSB average distance values for the test lines (physical and virtual) are obtained and compared with the mean distance error parameter. The average distance error value reaches maximum values of −2.6 μm in the pysical test line and 1.2 μm and 2.5 μm respectively in the virtual lines ($L1ks_2$ and $L1ks_3$). Additional error parameters calculated for each calibration point are the standard deviation of the TSB distance measurement error in the calibration and measurement processes with values under 0.6 μm for all the calibration points. Finally, the TSB expanded uncertainty U_i $(k = 2)$ for distance measurement in equation (7), is experimentally assessed for all the calibration points considering the measurement instrument under workshop conditions. The results do not exceed the 1.3 μm uncertainty value, both for the physical and virtual lines, increasing the uncertainty values with the distance measured. No big differences have been detected in the error parameter values among the three lines with distance method A.

In Table 3, the same distance comparison results for the TSB and the interferometer are presented but using distance calculation method B, see section 2.2.3, defining in this case a nominal distance of 40.5 mm between calibration point (i) and the following ($i + 1$). The results have been calculated from the data of ten iterations in eleven measurement points generating ten distances, D_i, with i from 1 to 10. The maximum average distance error value is −2.7 μm in the D_5 calibration point of the $L1ks_1$ test line. The standard deviation of the TSB distance measurement error in the calibration and measurement processes show a maximun value of 0.3 μm for all the calibration points and test lines. In regard to the TSB expanded uncertainty estimation for distance measurement for each calibration point in workshop conditions U_i $(k = 2)$, the maximum values are 0.8 μm, 0.7 μm and 0.7 μm for the physical test line and virtual lines $L1ks_2$ and $L1ks_3$ respectively. The values obtained with method B for all TSB distance error parameters and distance measurement uncertainties are slightly lower that with method A, due to the fact that the distances generated are bigger in method A (ranging from 40.5 mm to 405 mm) versus method B where it remains constant in 40.5 mm.

In Fig. 6 it is displayed in the TSB working volume, the TSB measurement expanded uncertainty U_i $(k = 2)$ for each calibration (i) point along the three test lines, with their distances defined according to method A and method B. The color bar (in mm) represents the expanded uncertainty values.

4. Conclusions

This work presented the evaluation procedure of a Telescopic Simultaneous Ballbar (TSB) with a reference interferometric equipment. One of the main TSB's applications is machine tool verification, allowing data capture in a single cycle thanks to the simultaneous operation of the three telescopic arms. Thus, the evaluation procedure was carried out in a 3-axis machine tool, measuring a test line along the MT's y-axis with both measurement equipment. The average distance error and its standard error deviation were the evaluation parameters chosen to compare the measurements made with the TSB and the interferometer. The distances among the points in the test line were defined with two methods (A and B) and an additional new methodology for virtual distances generation is proposed. The virtual lines enable to verify the behaviour of the TSB in a wider verification volume using single alignment position of the interferometer and MT position. The standard deviation of the distance error of the TSB in the calibration and measurement processes showed values under 0.6 μm for all the calibration points and the maximum average distance error ranges from 2.6 μm with distance generation method A to 2.7 μm with method B, obtaining comparable results. In addition, no significant differences were detected in the results obtained with the physical and the virtual test lines, showing the virtual methodology as a streamline approach.

The evaluation allows also to assess the TSB measurement expanded uncertainty in an experimental way under workshop conditions, showing uncertainty values below 1.3 μm with method A and 0.8 μm with method B, for all the calibration points defined in the test lines, both with the physical and virtual lines.

As a conclusion, the results obtained in the evaluation of the equipment proved the suitability of the TSB as measuring equipment for

Table 2
Mean error and uncertainty estimation for the measurement of distances with the TSB with method A.

Calibration Point	D_1	D_2	D_3	D_4	D_5	D_6	D_7	D_8	D_9	D_{10}
Nominal Distance/mm	40.5000	81.0000	121.5000	162.0000	202.5000	243.0000	283.5000	324.0000	364.5000	405.0000
U_{IFM} $(k_0 = 2)$/μm	0.5	0.5	0.5	0.5	0.5	0.5	0.5	0.5	0.5	0.5
L1ks1 -Test line										
IFM Mean/mm	40.5017	81.0090	121.5169	162.0211	202.5214	243.0255	283.5263	324.0257	364.5259	405.0280
TSB Mean/mm	40.5013	81.0078	121.5158	162.0201	202.5188	243.0242	283.5256	324.0251	364.5254	405.0277
Mean Error/μm	−0.4	−1.2	−1.1	−1.0	−2.6	−1.3	−0.7	−0.6	−0.5	−0.3
s_{ci} $(n_c = 10)$/μm	0.2	0.2	0.2	0.2	0.2	0.2	0.2	0.3	0.4	0.6
s_{mi} $(n_m = 1)$/μm	0.2	0.2	0.2	0.2	0.2	0.2	0.2	0.3	0.4	0.6
U_i $(k = 2)$/μm	0.6	0.7	0.7	0.7	0.7	0.7	0.6	0.8	0.9	1.3
L1ks2 - Virtual test line										
IFM Mean/mm	40.5061	81.0158	121.5261	162.0325	202.5365	243.0398	283.5408	324.0410	364.5416	405.0440
TSB Mean/mm	40.5060	81.0155	121.5259	162.0329	202.5371	243.0406	283.5416	324.0422	364.5428	405.0446
Mean Error/μm	−0.1	−0.3	−0.2	0.4	0.6	0.8	0.8	1.2	1.2	0.6
s_{ci} $(n_c = 10)$/μm	0.1	0.1	0.2	0.3	0.2	0.2	0.2	0.2	0.1	0.2
s_{mi} $(n_m = 1)$/μm	0.1	0.1	0.2	0.3	0.2	0.2	0.2	0.2	0.1	0.2
U_i $(k = 2)$/μm	0.5	0.5	0.6	0.7	0.7	0.6	0.7	0.6	0.5	0.6
L1ks3 - Virtual test line										
IFM Mean/mm	40.5052	81.0141	121.5224	162.0266	202.5295	243.0340	283.5350	324.0349	364.5353	405.0379
TSB Mean/mm	40.5050	81.0140	121.5224	162.0261	202.5294	243.0354	283.5370	324.0370	364.5377	405.0404
Mean Error/μm	−0.2	−0.1	0.0	−0.5	−0.1	1.4	2.0	2.1	2.4	2.5
s_{ci} $(n_c = 10)$/μm	0.2	0.3	0.4	0.4	0.4	0.3	0.5	0.5	0.5	0.6
s_{mi} $(n_m = 1)$/μm	0.2	0.3	0.4	0.4	0.4	0.3	0.5	0.5	0.5	0.6
U_i $(k = 2)$/μm	0.7	0.9	0.9	0.9	1.0	0.9	1.1	1.2	1.2	1.3

Table 3
Mean error and uncertainty estimation for the measurement of distances with the TSB with method B.

Calibration Point	D_1	D_2	D_3	D_4	D_5	D_6	D_7	D_8	D_9	D_{10}
Nominal Distance/mm	40.5000	40.5000	40.5000	40.5000	40.5000	40.5000	40.5000	40.5000	40.5000	40.5000
U_{IFM} (k_0 = 2)/μm	0.5	0.5	0.5	0.5	0.5	0.5	0.5	0.5	0.5	0.5
L1ks1 -Test line										
IFM Mean/mm	40.5017	40.5074	40.5079	40.5042	40.5004	40.5040	40.5008	40.4993	40.5003	40.5020
TSB Mean/mm	40.5013	40.5065	40.5081	40.5042	40.4976	40.5064	40.5014	40.4995	40.5003	40.5023
Mean Error/μm	0.4	0.9	−0.2	−0.1	2.7	−2.4	−0.6	−0.2	0.0	−0.3
s_{ci} (n_c = 10)/μm	0.2	0.2	0.3	0.1	0.2	0.3	0.2	0.2	0.3	0.3
s_{mi} (n_m = 1)/μm	0.2	0.2	0.3	0.1	0.2	0.3	0.2	0.2	0.3	0.3
U_i (k = 2)/μm	0.6	0.7	0.7	0.5	0.7	0.8	0.6	0.6	0.8	0.8
L1ks2 - Virtual test line										
IFM Mean/mm	40.5061	40.5097	40.5104	40.5064	40.5040	40.5033	40.5010	40.5002	40.5006	40.5023
TSB Mean/mm	40.5060	40.5095	40.5104	40.5070	40.5041	40.5035	40.5010	40.5006	40.5006	40.5018
Mean Error/μm	0.0	0.2	0.0	−0.7	−0.1	−0.2	0.0	−0.4	0.0	0.5
s_{ci} (n_c = 10)/μm	0.1	0.1	0.2	0.1	0.1	0.1	0.1	0.2	0.2	0.2
s_{mi} (n_m = 1)/μm	0.1	0.1	0.2	0.1	0.1	0.1	0.1	0.2	0.2	0.2
U_i (k = 2)/μm	0.5	0.6	0.7	0.6	0.5	0.5	0.5	0.7	0.6	0.6
L1ks3 - Virtual test line										
IFM Mean/mm	40.5052	40.5089	40.5083	40.5042	40.5029	40.5045	40.5010	40.4998	40.5004	40.5027
TSB Mean/mm	40.5050	40.5090	40.5084	40.5036	40.5033	40.5070	40.5016	40.4999	40.5007	40.5028
Mean Error/μm	0.2	−0.1	−0.1	0.5	−0.4	−2.5	−0.6	−0.1	−0.3	−0.1
s_{ci} (n_c = 10)/μm	0.2	0.2	0.1	0.1	0.1	0.2	0.2	0.1	0.1	0.1
s_{mi} (n_m = 1)/μm	0.2	0.2	0.1	0.1	0.1	0.2	0.2	0.1	0.1	0.1
U_i (k = 2)/μm	0.7	0.7	0.5	0.5	0.6	0.6	0.6	0.5	0.5	0.6

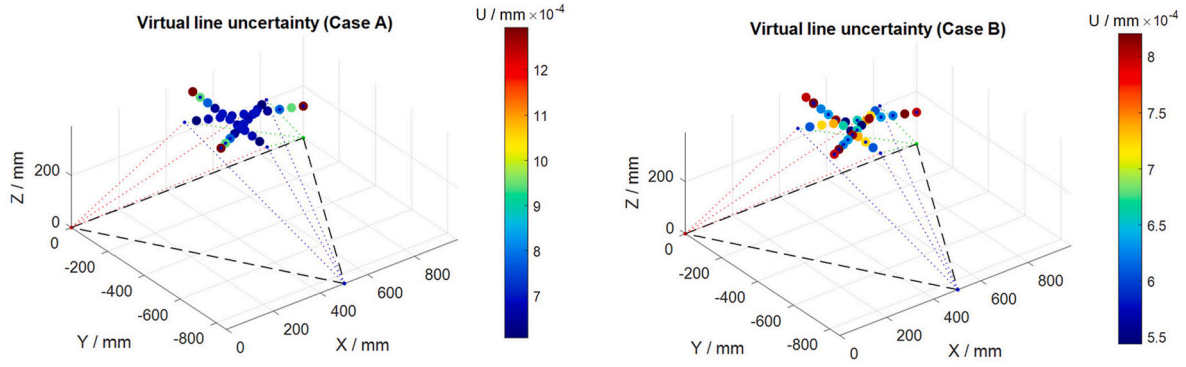

Fig. 6. TSB measurement expanded uncertainty U_i (k_i = 2) values (mm) in virtual lines measurement (a) Distance generation method A, (b) Distance generation method B.

machine tool verification considering the precision and repeatability required for the application, being the equipment accuracy levels assesed in the experimental evaluation close to those of laser interferometry.

Declaration of competing interest

The authors declare that they have no known competing financial interests or personal relationships that could have appeared to influence the work reported in this paper.

Acknowledgments

This research was funded by the Ministerio de Economía, Industria y Competitividad with project number Reto 2017-DPI2017-90106-R, by Aragon Government (Department of Industry and Innovation) through the Research Activity Grant for research groups recognized by the Aragon Government (T56_17R Manufacturing Engineering and Advanced Metrology Group). This is co-funded with European Union ERDF funds (European Regional Development Fund 2014–2020, "Construyendo Europa desde Aragón"). Authors would like to acknowledge the use of Servicio General de Apoyo a la Investigación-SAI, Universidad de Zaragoza.

References

[1] Gao W, Ibaraki S, Donmez MA, Kono D, Mayer JRR, Chen YL, et al. Machine tool calibration: measurement, modeling, and compensation of machine tool errors. Int J Mach Tool Manufact 2023;187:104017. https://doi.org/10.1016/J.IJMACHTOOLS.2023.104017.
[2] Slocum AH. Precision machine design. Prentice Hall; 1992.
[3] Zhang Z, Jiang F, Luo M, Wu B, Zhang D, Tang K. Geometric error measuring, modeling, and compensation for CNC machine tools: a review. Chin J Aeronaut 2023. https://doi.org/10.1016/J.CJA.2023.02.035.
[4] Gao W, Kim SW, Bosse H, Haitjema H, Chen YL, Lu XD, et al. Measurement technologies for precision positioning. CIRP Ann - Manuf Technol 2015;64:773–96. https://doi.org/10.1016/j.cirp.2015.05.009.
[5] International Organization for Standardization. ISO 230-1:2012. Test code for machine tools — Part 1: geometric accuracy of machines operating under no-load or quasi-static conditions. 2012.
[6] Kunzmann H, Trapet E, Wäldele F. A uniform concept for calibration, acceptance test, and periodic inspection of coordinate measuring machines using reference objects. CIRP Ann Technol 1990;39:561–4.
[7] Breitzke A, Wolfgang H. Workshop-suited geometric errors identification of three-axis machine tools using on-machine measurement for long term precision assurance. Precis Eng 2022;75:235–47. https://doi.org/10.1016/j.precisioneng.2022.02.006.
[8] Belforte G, Bona B, Canuto E, Donati F, Ferraris F, Gorini I, et al. Coordinate measuring machines and machine tools selfcalibration and error correction. CIRP Ann 1987;36:359–64. https://doi.org/10.1016/S0007-8506(07)62622-5.
[9] Schwenke H, Knapp W, Haitjema H, Weckenmann A, Schmitt R, Delbressine F. Geometric error measurement and compensation of machines—an update. CIRP Ann 2008;57:660–75. https://doi.org/10.1016/j.cirp.2008.09.008.
[10] Florussen GHJ, Delbressine FLM, Van De Molengraft MJG, Schellekens PHJ. Assessing geometrical errors of multi-axis machines by three-dimensional length

measurements. Measurement 2001;30:241–55. https://doi.org/10.1016/S0263-2241(01)00016-1.
[11] Aguado S, Samper D, Santolaria J, Aguilar JJ. Machine tool rotary Axis compensation trough volumetric verification using laser tracker. Procedia Eng 2013;63:582–90. https://doi.org/10.1016/j.proeng.2013.08.189.
[12] Aguado S, Samper D, Santolaria J, Aguilar JJ. Identification strategy of error parameter in volumetric error compensation of machine tool based on laser tracker measurements. Int J Mach Tool Manufact 2012;53:160–9. https://doi.org/10.1016/j.ijmachtools.2011.11.004.
[13] Qiao Y, Chen Y, Yang J, Chen B. A five-axis geometric errors calibration model based on the common perpendicular line (CPL) transformation using the product of exponentials (POE) formula. Int J Mach Tool Manufact 2017;118–119:49–60. https://doi.org/10.1016/j.ijmachtools.2017.04.003.
[14] Wan A, Wang Y, Xue G, Chen K, Xu J. Accurate kinematics calibration method for a large-scale machine tool. IEEE Trans Ind Electron 2020;46. https://doi.org/10.1109/tie.2020.3021657. 1–1.
[15] Mchichi NA, Mayer JRR. Optimal calibration strategy for a five-axis machine tool accuracy improvement using the D-optimal approach. Int J Adv Manuf Technol 2019;103:251–65. https://doi.org/10.1007/s00170-019-03454-2.
[16] Xing K, Achiche S, Mayer JRR. Five-axis machine tools accuracy condition monitoring based on volumetric errors and vector similarity measures. Int J Mach Tool Manufact 2019;138:80–93. https://doi.org/10.1016/j.ijmachtools.2018.12.002.
[17] Xiang S, Deng M, Li H, Du Z, Yang J. Volumetric error compensation model for five-axis machine tools considering effects of rotation tool center point. Int J Adv Manuf Technol 2019;102:4371–82. https://doi.org/10.1007/s00170-019-03497-5.
[18] Esmaeili SM, Mayer JRR, Sanders MP, Dahlem JP, Xing K. Five-Axis machine tool volumetric and geometric error reduction by indirect geometric calibration and lookup tables. J Manuf Sci Eng 2021;143:1–14. https://doi.org/10.1115/1.4049846.
[19] Li J, Mei B, Shuai C, Liu X, Liu D. A volumetric positioning error compensation method for five-axis machine tools. Int J Adv Manuf Technol 2019;103:3979–89. https://doi.org/10.1007/s00170-019-03745-8.
[20] Aguado S, Pérez P, Albajez JA, Velázquez J, Santolaria J. Inaccuracy of machine tools due to verification conditions. Meas J Int Meas Confed 2022;188. https://doi.org/10.1016/j.measurement.2021.110629.
[21] Ramesh R, Mannan MA, Poo AN. Error compensation in machine tools — a review: Part II: thermal errors. Int J Mach Tool Manufact 2000;40:1257–84. https://doi.org/10.1016/S0890-6955(00)00010-9.
[22] Li Y, Zhao W, Lan S, Ni J, Wu W, Lu B. A review on spindle thermal error compensation in machine tools. Int J Mach Tool Manufact 2015;95:20–38. https://doi.org/10.1016/J.IJMACHTOOLS.2015.04.008.
[23] Holub M, Andrs O, Kovar J, Vetiska J. Effect of position of temperature sensors on the resulting volumetric accuracy of the machine tool. Measurement 2020;150:107074. https://doi.org/10.1016/J.MEASUREMENT.2019.107074.
[24] Aguado Pérez, Albajez, Santolaria, Velázquez. Study on machine tool positioning uncertainty due to volumetric verification. Sensors 2019;19:2847. https://doi.org/10.3390/s19132847.
[25] Aguado S, Santolaria J, Samper D, Velazquez J, Aguilar JJ. Empirical analysis of the efficient use of geometric error identification in a machine tool by tracking measurement techniques. Meas Sci Technol 2016;27:035002. https://doi.org/10.1088/0957-0233/27/3/035002.
[26] Zha J, Wang T, Li L, Chen Y. Volumetric error compensation of machine tool using laser tracer and machining verification. Int J Adv Manuf Technol 2020;108:2467–81. https://doi.org/10.1007/s00170-020-05556-8.
[27] Holub M, Andrs O, Kovar J, Vetiska J. Effect of position of temperature sensors on the resulting volumetric accuracy of the machine tool. Measurement 2020;150:107074. https://doi.org/10.1016/j.measurement.2019.107074.
[28] Wang J, Guo J. The identification method of the relative position relationship between the rotary and linear axis of multi-axis numerical control machine tool by laser tracker. Meas J Int Meas Confed 2019;132:369–76. https://doi.org/10.1016/j.measurement.2018.09.062.
[29] Li Q, Wang W, Zhang J, Shen R, Li H, Jiang Z. Measurement method for volumetric error of five-axis machine tool considering measurement point distribution and adaptive identification process. Int J Mach Tool Manufact 2019;147:103465. https://doi.org/10.1016/j.ijmachtools.2019.103465.
[30] Wang JD, Wang QJ, Li HT. The method of geometric error measurement of NC machine tool based on the principle of space vector's direction measurement. Int J Precis Eng Manuf 2019;20:511–24. https://doi.org/10.1007/s12541-019-00062-8.
[31] Aguado S, Santolaria J, Samper D, Aguilar JJ. Study of self-calibration and multilateration in machine tool volumetric verification for laser tracker error reduction. Proc Inst Mech Eng Part B J Eng Manuf 2014;228. https://doi.org/10.1177/0954405413511074.
[32] Aguado S, Santolaria J, Samper D, José Aguilar J. Forecasting method in multilateration accuracy based on laser tracker measurement. Meas Sci Technol 2017;28. https://doi.org/10.1088/1361-6501/aa5073.
[33] Linares JM, Arroyave-Tobon S, Pires J, Sprauel JM. Effects of number of digits in large-scale multilateration. Precis Eng 2020;64:1–6. https://doi.org/10.1016/j.precisioneng.2020.03.009.
[34] Deng M, Li H, Xiang S, Liu P, Feng X, Du Z, et al. Geometric errors identification considering rigid-body motion constraint for rotary axis of multi-axis machine tool using a tracking interferometer. Int J Mach Tool Manufact 2020;158:103625. https://doi.org/10.1016/j.ijmachtools.2020.103625.
[35] Ibaraki S, Kudo T, Yano T, Takatsuji T, Osawa S, Sato O. Estimation of three-dimensional volumetric errors of machining centers by a tracking interferometer. Precis Eng 2015;39:179–86. https://doi.org/10.1016/J.PRECISIONENG.2014.08.007.
[36] Deng M, Feng X, Du Z. Non-redundant identification of geometric errors in multilateration of rotary axis. Int J Mech Sci 2023;256:108529. https://doi.org/10.1016/J.IJMECSCI.2023.108529.
[37] ETALON. Etalon X-AX LASERBAR. The system solution for calibration, compensation and verification of small and middle size machine tools. 2019.
[38] Thiel Jutta. Squeezing out the last micron. Optik&Photonics 2014;2:55–7.
[39] Liu CS, Hsu HC, Lin YX. Design of a six-degree-of-freedom geometric errors measurement system for a rotary axis of a machine tool. Opt Laser Eng 2020;127:105949. https://doi.org/10.1016/j.optlaseng.2019.105949.
[40] Gao W, Weng L, Zhang J, Tian W, Zhang G, Zheng Y, et al. An improved machine tool volumetric error compensation method based on linear and squareness error correction method. Int J Adv Manuf Technol 2020;106:4731–44. https://doi.org/10.1007/s00170-020-04965-z.
[41] Jiang X, Wang L, Liu C. Geometric accuracy evaluation during coordinated motion of rotary axes of a five-axis machine tool. Meas J Int Meas Confed 2019;146:403–10. https://doi.org/10.1016/j.measurement.2019.03.060.
[42] Jae Pahk H, Sam Kim Y, Hee Moon J. A new technique for volumetric error assessment of CNC machine tools incorporating ball bar measurement and 3D volumetric error model. Int J Mach Tool Manufact 1997;37:1583–96. https://doi.org/10.1016/S0890-6955(97)00029-1.
[43] Zhong L, Bi Q, Wang Y. Volumetric accuracy evaluation for five-axis machine tools by modeling spherical deviation based on double ball-bar kinematic test. Int J Mach Tool Manufact 2017;122:106–19. https://doi.org/10.1016/J.IJMACHTOOLS.2017.06.005.
[44] Weikert S, Knapp W. R-test, a new device for accuracy measurements on five axis machine tools. CIRP Ann - Manuf Technol 2004;53:429–32. https://doi.org/10.1016/S0007-8506(07)60732-X.
[45] Hong C, Ibaraki S. Non-contact R-test with laser displacement sensors for error calibration of five-axis machine tools. Precis Eng 2013;37:159–71. https://doi.org/10.1016/J.PRECISIONENG.2012.07.012.
[46] Aguilar JJ, Acero R, Brosed FJ, Santolaria J. Development of a high precision telescopic instrument based on simultaneous laser multilateration for machine tool volumetric verification. Sensors 2020;20:3798. https://doi.org/10.3390/s20133798.
[47] Acero R, Aguilar JJ, Brosed FJ, Santolaria J, Aguado S, Pueo M. Design of a multi-point kinematic coupling for a high precision telescopic simultaneous measurement system. Sensors 2021;21:6365. https://doi.org/10.3390/s21196365.
[48] Verein Deutscher Ingenieure. VDI/VDE 2617 Part 10. Acceptance and reverification tests of laser tracker, vols. 1–36; 2011.
[49] UNE Asociación Española de Normalización. UNE-EN ISO 10360-10 Geometrical product specifications (GPS) Acceptance and reverification tests for coordinate measuring systems (CMS) Part 10. Laser trackers; 2023.
[50] Brosed FJ, Cacho RA, Aguado S, Herrer M, Aguilar JJ, Mazo JS. Development and validation of a calibration gauge for length measurement systems. Materials 2019;12. https://doi.org/10.3390/ma122333960.
[51] Brosed FJ, Aguilar JJ, Acero R, Santolaria J, Aguado S, Pueo M. Calibration and uncertainty budget analysis of a high precision telescopic instrument for simultaneous laser multilateration. Measurement 2022;190:110735. https://doi.org/10.1016/j.measurement.2022.110735.
[52] Aguado S, Brosed FJ, Acero R, Aguilar JJ, Santolaria J, Pueo M. Influence of high precision telescopic instrument characterization on multilateration points accuracy. IOP Conf Ser Mater Sci Eng 2021;1193:012061. https://doi.org/10.1088/1757-899X/1193/1/012061.
[53] Joint Committee for Guides in Metrology. Evaluation of measurement data: guide to the expression of uncertainty in measurement. 2008. https://doi.org/10.1373/clinchem.2003.030528.